BONDS NDE USING STIMULATED INFRARED THERMOGRAPHY

P.M. Delpech, D.M. Boscher, F. Lepoutre,
A.A. Déom and D.L. Balageas

Office National d'Etudes et de Recherches Aérospatiales (ONERA)
Division de Thermophysique
29 avenue de la Division Leclerc
Châtillon, France 92320

INTRODUCTION

Among all the photothermal techniques that have appeared since some years , the photothermal radiometry is very attractive because of its noncontact and rapid-scanning ability [1,2]. In our laboratory, we developed pulsed stimulated infrared (IR) thermography [3]. Due to the relatively low refreshment frequency of the currently used IR cameras, the application of the method was restricted to low thermal conductors. In particular, we applied it to carbon/epoxy composites [4,5]. Some new developments of the data reduction procedure were presented last year [6] to use this technique with good heat conductors. Satisfactory results were obtained in the case of delaminations in C/C composites. We present here an improvement of this data reduction procedure which is able now to work with any kind of material. We will focus our attention on the especially difficult case of the characterization of adhesive joints in metallic structures.

The new data reduction procedure is explained in the second section and tested on aluminium samples containing calibrated air gaps. This test proves that this method is able to work quantitatively in real time. Finally in the last section, we present the application of this procedure to metal-metal stuck lap joints samples. In these metallic samples, the two-dimentional effects (2-D) are often present and can strongly modify the thermal resistance images. Nevertheless, we will show that our monodimensional (1-D) procedure is able to identify rather reliable information.

DATA REDUCTION PROCEDURE FOR GOOD CONDUCTORS

The isothermal model

Let us consider a two layer sample of total thickness e, with a non perfect thermal contact at the interface, located at a depth e_1 (see fig. 1a). We set:
$e_2 = e-e_1$, and C_1, C_2 the volumic heat capacities of the first and second layers respectively. At every time after the pulsed heat deposition, the temperature distribution can be represented by the sketch of fig. 1b. If we take into account the fact that the thermal resistance of the defect is much larger than the thermal resistances of the two layers (which have high conductivities), each layer may be considered as isothermal, with temperatures $T_1(t)$ in the first layer and $T_2(t)$ in the second one. With these assumptions, the energy conservation leads to the following equations:

$$C_1 e_1 \frac{dT_1}{dt} = -\frac{1}{R}(T_1-T_2) = -C_2 e_2 \frac{dT_2}{dt} \quad , \qquad (1)$$

Review of Progress in Quantitative Nondestructive Evaluation, Vol. 11
Edited by D.O. Thompson and D.E. Chimenti, Plenum Press, New York, 1992

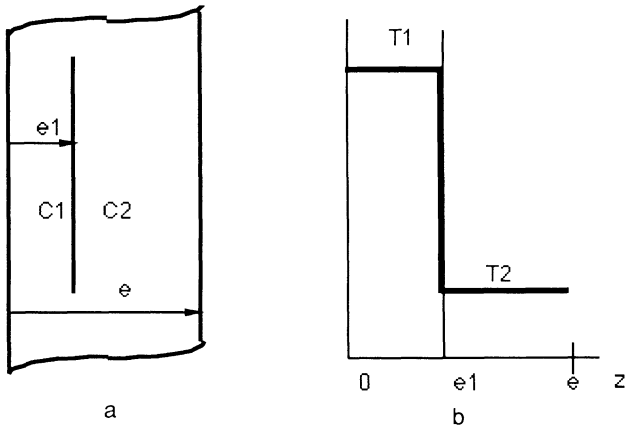

Fig. 1. Model used for defect identification in the case of high conductive materials.
a. Sample composed of two layers (subscript 1 and 2) with non perfect contact at the interface located at depth e_1.
b. Temperature profile in the sample of fig. 1.a after a pulsed heat deposition at z=0.

$$C_1e_1T_1+C_2e_2T_2 = Q\,, \qquad (2)$$

in which Q is the fluence.

In the case of a Dirac heat pulse, the initial temperatures (t=0) in the two layers are :

$T_1(t=0) = Q / C_1 e_1, \quad T_2(t=0) = 0.$

Using equations (1) and (2), one obtains:

$$C_1e_1\frac{dT_1}{dt} + \frac{1}{R}\,\frac{C_1e_1+C_2e_2}{C_2e_2}\,T_1 = \frac{Q}{RC_2e_2}\,,$$

the solution of which is :

$$T_{1D}(t) = \frac{Q}{C_1e_1+C_2e_2}\left[1+\frac{C_2e_2}{C_1e_1}\exp\left(-\frac{C_1e_1+C_2e_2}{RC_1e_1C_2e_2}\,t\right)\right]. \qquad (3)$$

This solution can be extended to the case of a square pulse of finite duration τ (Duhamel theorem) and this extended temperature T_1 can be normalized (T_1^*) using the temperature $T_{1\infty}$ reached at very large times with no heat losses :

$$T_{1\infty} \approx \frac{Q}{C_1e_1+C_2e_2}\,,$$

$$T_1^* = \frac{T_1-T_{1\infty}}{T_{1\infty}} = \frac{R}{\tau}\,\frac{(C_2e_2)^2}{C_1e_1+C_2e_2}\left[\exp\left(\frac{C_1e_1+C_2e_2}{RC_1e_1C_2e_2}\,\tau\right)-1\right]\exp\left(-\frac{C_1e_1+C_2e_2}{RC_1e_1C_2e_2}\,t\right) \qquad (4)$$

A data reduction procedure can be proposed for the identification of the depth e_1 and the thermal resistance R of the bond. According to eq. (4), the thermogram (see figure 2), in semilogarithmic scale, $\mathrm{Log}(T_1^*)=\mathrm{Log}(T_1^*(t=0))+st$, is a straight line of slope s, $s=-(C_1e_1+C_2e_2)/RC_1e_1C_2e_2$ and of ordinate at the origin :

$$T_1^*(0) = \frac{R}{\tau}\,\frac{(C_2e_2)^2}{C_1e_1+C_2e_2}\left[\exp\left(\frac{C_1e_1+C_2e_2}{RC_1e_1C_2e_2}\,\tau\right)-1\right].$$

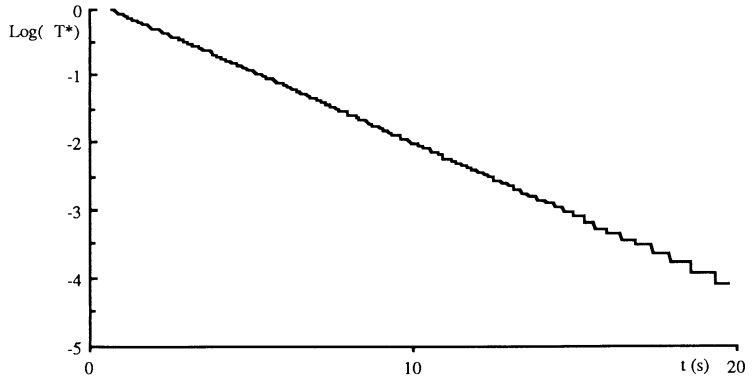

Fig. 2. Semi-logarithmic representation of the normalized temperature at the surface of the sample as a function of time

The depth of the interface verifies the relation :

$$e_1 = \frac{e}{1+\frac{C_1}{C_2}\,\tau\,\frac{T_1^*(0)\ s}{K}} \quad \text{with } K = \exp\left(\frac{C_1e_1+C_2e_2}{RC_1e_1C_2e_2}\,\tau\right)-1,$$

which allows an iterative determination of the depth e_1, once s and $T_1^*(t=0)$ have been experimentally determined on the graph $\mathrm{Log}T_1^* = f(t)$. The procedure starts with the value $e_1 = e/2$ and stops when two successive values are close enough. In practice, five iterations are sufficient for a convergence better than 10^{-3}. Finally, the thermal resistance R characterizing the bond is given by the relation:

$$R = \frac{C_1e_1+C_2e_2}{sC_1e_1C_2e_2}\ .$$

Let us note that generally e_1 is known and there is just to identify R.

Procedure to reach the adiabatic temperature $T_{1\infty}$

Let us recall that to use the very simple feature of figure 2, it is necessary to reach the experimental value of $T_{1\infty}$. Pratically $T_{1\infty}$ cannot be determined directly from the thermogram because the caracteristic time of convective losses is of the order of a few tens of seconds. Thus, the experiment must not exceed this time and typically we used 20 seconds. But, if the thermal resistance of the bond is important the adiabatic temperature is not reached at this time.

Actually, it is always possible to determine $T_{1\infty}$ from the temperature $T_1(t)$ at any time t provided that, (i) heat losses have not affected $T_1(t)$ and, (ii) the signal to noise ratio is large enough. To improve the first point (i), we stop the analysis of the thermogram at a time t_{max}. It is difficult to find a universal criterion for the choice of t_{max}. Generally we look at the thermogram of a particular pixel and we choose t_{max} as the limit over which a decrease characteristic of the beginning of the heat losses appears. To improve the second point (ii), let us recall that our experimental thermogram is given by :

$$T_1(t) = a + b\ .e^{(-c.t)} \qquad (5)$$

from which we have to deduce a, b and c.

If we call T_{1max} the temperature at $t = t_{max}$, we can write :

$$\Delta T = T - T_{max} = b\ .(\ e^{(-c.t)} - e^{(-c.tmax)}\ ) \qquad (6)$$

which is a function of only b and c .

Now we calculate a weighted integral of ΔT :

$$I = \int_{t_{min}}^{t_{max}} \Delta T \; e^{(-p.t)} \, dt \qquad (7)$$

in which t_{min} is roughly the time of the end of the heat pulse.

The purpose of this integral is to reduce the noise by increasing the weight of the temperature at the beginning of the thermogram and, on the contrary, to decrease the weight at the end of the thermogram which is much more noisy.

Finally to eliminate b from equation (7), it is necessary to evaluate I for two values of p (p_1 and p_2) and to calculate the ratio $I(p_1)/I(p_2)$ which depends only on c. The choice of p_1 and p_2 is not critical, but these two values must be chosen as different as possible, keeping in mind that if p_2 is too large the calculation of $I(p_2)$ will not be an exact integral but, actually, a finite sum of a few images : we generally take $p_1 = 1/t_{max}$ and $p_2 = 2p_1$. We have shown with numerical simulation that this procedure reproduces quite well the complete thermogram even if $T_{1\infty}$ is experimentally totally unknown.

Experimental check of the data reduction

Our procedure is normally efficient if the 1-D assumption is verified. We have prepared a sample made of two 1 mm thick Al plates separated by a known calibrated air gap varying from 10 to 120 µm (± 10 µm) (see Fig.3a). The surface of the sample covered by a black paint was illuminated uniformly by the heat source [3,6]. The IR images were recorded during 20 s and the data reduction procedure was applied to each pixel. Figures 3 b and c give images of the depth location of the air gap (in µm) and of the thermal resistance (air gap thickness in µm).

The two images are in very good agreement with the geometry of the sample. Note that these images are not a complete view of the sample but are limited to the part in which the air gap thickness varies between 40 and 120 µm. We can now use our system for real stuck samples.

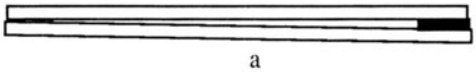

a

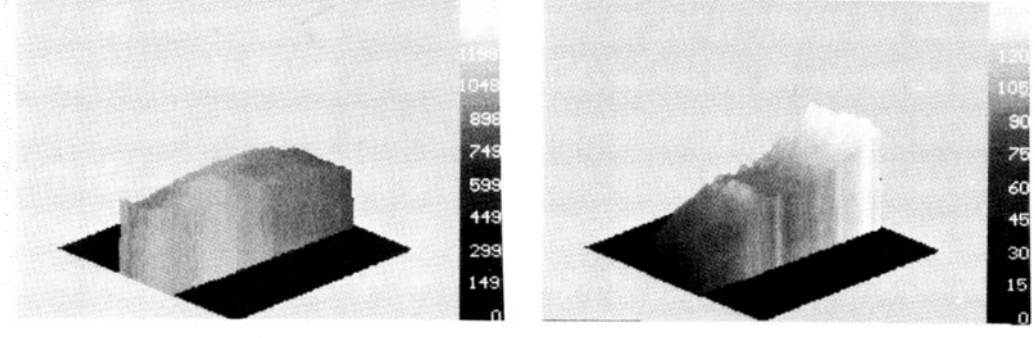

b c

Fig.3. Sample made of two aluminium plates (1mm thick) separated by a corner of air.
a. Schematic cross section of the sample. The air gap thickness increases from 10µm to 120µm .
b. Location of the air gap (in µm) beneath the surface.
c. Thermal resistance of the air gap expressed in thickness of air (µm).

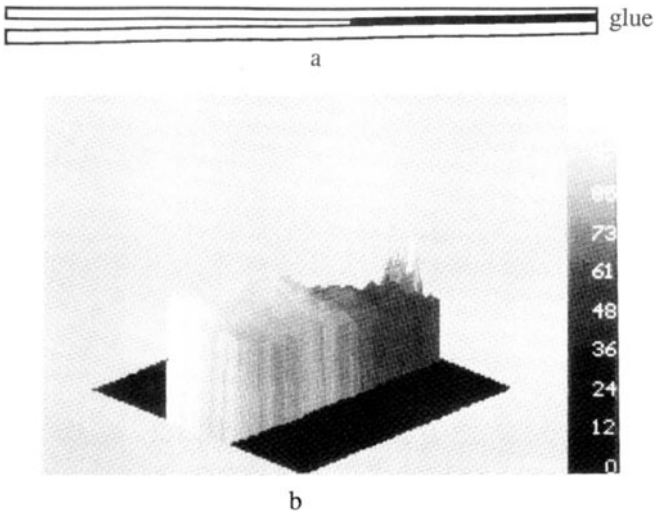

Fig. 4. Sample made of two aluminium plates (1mm thick) partially stuck with a very thin slab of glue.
a. Schematic cross section of the sample. The thickness of the glue is less than 10μm, the thickness of the air gap in the middle of the sample is equal to 100μm.
b. Thermal resistance of the air gap expressed in thickness of air (μm).

QUANTITATIVE IMAGES OF AIR GAPS IN ALUMINIUM STUCK SAMPLES

We prepared samples of aluminium AG5 made of two flat sheets (1 mm thick) stuck together with Cyanolit® glue. The stuck area represents approximately 30 percent of the total surface. The thickness of the glue cannot be measured precisely but is certainly less than 10 μm. It must be noticed that this glue is quite porous. A thickness of 100 μm of the air gap was measured in the middle of the part which is non stuck using a metallographic microscope (see Fig.4a).

Figure 4 gives the thermal resistance image obtained using the data reduction described in section 2. The low thermal resistance appearing in the upper part corresponds to the stuck area while in the bottom of the figure, the value of the air gap thickness is in good agreement with the microscopic measurements. It must be noticed that the thermal resistance determined in the stuck area seems to be too large taking into account the fact that the glue is very thin and its thermal conductivity is, at least, ten times larger than the one of air. We have attributed this disagreement to the large amount of air included in the stuck part.

Finally, we prepared a few stuck samples of aluminium AG5 flat sheets with a reinforced stick film used in aeronautical industry (Ciba®). The thickness of the glue was measured with a metallographic microscope and we found 400μm on one side of the sample and 100μm on the other side. A lack of glue was created in the center of the sample. Once again, the method described previously was used and images in thermal resistance were obtained.

Figure 5 gives the thermal resistance images obtained by decreasing the value of the time t_{max} at which we stopped the data reduction. From left to right of figure 5 we took t_{max} = 16 s, 12 s and 8 s. For the two largest times t_{max}, the lack of glue does not appear clearly while it is quite well revealed at t_{max} = 8 s. This effect is due to the high conductivity of Aluminium which produces a 2-D heat flow at times larger than ten seconds and then totally hides the structure of the defect. This result shows that our 1-D procedure is able to provide a qualitative 2-D image provided that good thermograms can be recorded at short times. But actually the procedure does not give the exact value of the thermal resistance: for instance we do not see on figure 5 the variation of the thickness of the air gap in the unstuck area as one goes from the left side to the right side (which was present in the sample due to the fact that we used two different thicknesses of glue on the two stuck sides).

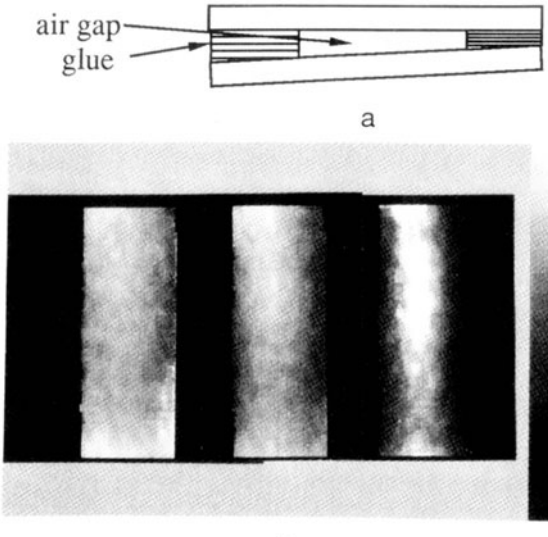

Fig. 5 Sample made of two aluminium plates (1mm thick) partially stuck with calibrated slabs of glue on its two sides.
a. Schematic cross section of the sample. The thickness of the glue is equal to 100µm on the right side and 400µm on the left side. The thickness of the air gap in the middle of the sample cannot be measured.
b. Thermal resistance of the air gap expressed in thickness of air (µm).

CONCLUSION

We described a monodimensional data reduction of IR camera images to provide in real time the values of the depth profile and the thermal resistance of bonds in metallic stuctures.

The method is quantitative when the lateral heat diffusion extension is small compared to the surface occupied by the defects. If the unbonded regions are located on small areas, it is still possible to obtain the location of the thermal resistances, but their values are strongly affected by the 2-D effects. It is then necessary to use a more sophisticated model which is still in progress in our laboratory to remain compatible with a short time processing.

REFERENCES

1. P. Cielo, R. Lewak, and D.L. Balageas, in Thermosense VIII, edited by H. Kaplan (SPIE, Belingham, WA, 1986), Vol. 581, pp. 47-54.
2. P. Cielo, X. Maldague, A.A. Déom, and R. Lewak, Materials Evaluations 45, 452 (1987).
3. P. Potet, D.L. Balageas, A.A. Déom, and D.M. Boscher, in Review of progress in Quantitative NDE, edited by D.O. Thompson and D.E. Chimenti (Plenum Press, New York, 1990), Vol. 9A, pp. 1017-1023.
4. D.L. Balageas, A.A. Déom, and D.M. Boscher, Materials Evaluations 45, 461 (1987).
5. A.A. Déom, D.M. Boscher, and D.L. Balageas, in Review of progress in Quantitative NDE, edited by D.O. Thompson and D.E. Chimenti (Plenum Press, New York, 1990), Vol. 9A, pp. 525-531.
6. D.L. Balageas, P.M. Delpech, D. Boscher and A. Deom, in Review of Progress in Quantitative Non Destructive Evaluation, edited by D.O. Thompson and D.E. Chimenti (Plenum Press, New York, 1991), Vol. 10B, pp. 1073-1081.